Journal of Nuclear Materials 465 (2015) 682–691

Contents lists available at ScienceDirect

Journal of Nuclear Materials

journal homepage: www.elsevier.com/locate/jnucmat

Thermochemistry of rare earth doped uranium oxides $Ln_xU_{1-x}O_{2-0.5x+y}$ (Ln = La, Y, Nd)

Lei Zhang, Alexandra Navrotsky*

Peter A. Rock Thermochemistry Laboratory and NEAT ORU and Department of Chemical Engineering and Materials Science, University of California Davis, Davis, CA, 95616, USA

ARTICLE INFO

Article history:
Received 18 March 2015
Received in revised form
29 May 2015
Accepted 30 June 2015
Available online 6 July 2015

Keywords:
Thermochemistry
Doped uranium oxide
Formation enthalpy

ABSTRACT

Lanthanum, yttrium, and neodymium doped uranium dioxide samples in the fluorite structure have been synthesized, characterized in terms of metal ratio and oxygen content, and their enthalpies of formation measured by high temperature oxide melt solution calorimetry. For oxides doped with 10–50 mol % rare earth (Ln) cations, the formation enthalpies from constituent oxides ($LnO_{1.5}$, UO_2 and UO_3 in a reaction not involving oxidation or reduction) become increasingly exothermic with increasing rare earth content, while showing no significant dependence on the varying uranium oxidation state. The oxidation enthalpy of $Ln_xU_{1-x}O_{2-0.5x+y}$ is similar to that of UO_2 to UO_3 for all three rare earth doped systems. Though this may suggest that the oxidized uranium in these systems is energetically similar to that in the hexavalent state, thermochemical data alone can not constrain whether the uranium is present as U^{5+}, U^{6+}, or a mixture of oxidation states. The formation enthalpies from elements calculated from the calorimetric data are generally consistent with those from free energy measurements.

1. Introduction

UO_2 containing the fissile isotope U-235 is used in fuel rods in nuclear reactors, taking advantage of its high melting point [1]. Uranium dioxide crystallizes in the fluorite structure up to its melting point. During the burning of nuclear fuel, fission products are generated in amounts that depend on the composition of the fuel, the type of reactor, and the length of time the fuel is used [2]. The thermodynamic behavior of nuclear fuel during fission and irradiation is therefore crucial for understanding the stability of the fuel in operation, the modeling of storage and eventual disposal or reprocessing.

The incorporation of the fission products into the UO_2 fluorite structure has been studied over the decades [4]. Among the various fission products, rare earth (lanthanide, Ln) oxides have high yield and can form solid solutions with the host oxide over a wide composition range. Neodymium is the major rare earth fission product, followed by lanthanum and yttrium [5]. Large solubility limits are reported for lanthanides in UO_2: 82 mol % for $LaO_{1.5}$ [6], 65 mol % for $NdO_{1.5}$, and 48 mol % for $YO_{1.5}$ [7]. The addition of lanthanum has been reported to stabilize the fluorite structure under oxidizing condition and prevent its oxidation to U_3O_8, which would be accompanied by a destructive bulk expansion [8].

Knowledge of thermodynamics of these lanthanide doped fuel oxides is also crucial for the development of waste forms for immobilizing actinides. Direct disposal is adopted by several countries including the United States, in which the spent nuclear fuel is transferred to temporary or permanent storage, possibly in deep geological repositories [9]. The immobilization of nuclear waste requires a stable and durable material which also prevents the separation of the radionuclides from the matrix. A number of specific materials, both glass and ceramic, has been developed to host the waste, while UO_2 itself has been proposed to be a potential phase for immobilization as well [10,11]. Thermodynamics of these materials is therefore important for waste form development.

Most earlier thermodynamic data were obtained by measuring oxygen potential of fluorite solid solutions between uranium dioxide and trivalent rare earth oxides [3,12–15]. Separating such free energies into their enthalpy and entropy components is difficult because of the changing oxygen stoichiometry of the solid solutions, the high temperature and relatively small accessible temperature range over which equilibrium can be maintained, and the complexity of possible temperature dependent order – disorder reactions. Until recently, direct calorimetric measurements of

* Corresponding author.
E-mail address: anavrotsky@ucdavis.edu (A. Navrotsky).

http://dx.doi.org/10.1016/j.jnucmat.2015.06.059
0022-3115/

enthalpies of formation were not reported, mostly due to the refractory nature of the materials. Mazeina et al. performed the first direct measurements by high temperature oxide melt solution calorimetry of the enthalpy of formation in the solid solutions of $UO_{2\pm x}$ with CaO and $YO_{1.5}$ [16].

The rare earth doped UO_2 systems are complex due to the presence of oxygen vacancies in order to accommodate the substitution of U^{4+} by Ln^{3+}, and multiple possible stoichiometries due to the oxidation of U^{4+} to U^{5+} and/or U^{6+}. Indeed, especially at low dopant concentrations, oxygen excess (as interstitials) as well as oxygen deficiency (as vacancies) can occur [3]. Not only is the stoichiometry of the doped oxide hard to control during sintering, but it is also a challenge to accurately determine the oxygen content, related to the formal U^{4+}/U^{6+} ratio [17]. It is found that the oxygen potential of rare earth doped $UO_{2\pm x}$ increases with the oxygen/metal ratio at all temperatures and with increasing dopant content at relatively low concentration. These changes are most significant near O/M = 2 [12–15]. The doped uranium dioxide thus has a large tendency to oxidize toward the MO_2 stoichiometric composition even at very low oxygen partial pressure to compensate the trivalent lanthanide defects in competition with the creation of oxygen vacancies. Therefore new methods to prepare the solid solution close to the $Ln_xU_{1-x}O_{2-0.5x}$ stoichiometry, as well as accurate determination of the oxygen content of the samples, need to be developed in order to provide well characterized samples for thermochemical studies.

In this paper, we report the synthesis, characterization, and measurement of enthalpies of formation for $Ln_xU_{1-x}O_{2-0.5x+y}$ solid solutions from oxides by high temperature oxide melt solution calorimetry for lanthanum, yttrium, and neodymium doped uranium oxide. The compositions of the samples prepared here are $0 < x < 0.5$, with various oxygen contents for similar dopant concentration.

2. Experimental procedures

2.1. Syntheses

A coprecipitation method for the synthesis of lanthanide doped urania solid solutions was used [18,19]. Appropriate amounts of uranium nitrate ($UO_2(NO_3)_2\cdot 6H_2O$), and rare earth nitrate hexahydrate ($La(NO_3)_3\cdot 6H_2O$, $Y(NO_3)_3\cdot 6H_2O$, $Nd(NO_3)_3\cdot 6H_2O$) were mixed and then dissolved in deionized water. After complete dissolution, excess NH_4OH was added to the solution until it reached a pH of 9–10 to allow the precipitate to form. The mixture was stirred and heated on a hot plate at about 80 °C for several days to decrease the solution volume. Then the remaining solution was transferred into a platinum crucible to a furnace for drying in air at 150 °C overnight, followed by calcination in air at 600 °C for 6 h. The powder was then ground in an agate mortar and pressed into pellets 5 mm in diameter for further sintering. The Ln-doped uranium oxide pellets were sintered in alumina crucibles at various temperatures from 1100 to 1450 °C for 24–36 h in a reducing atmosphere, 5% H_2 in Ar, to achieve homogeneous bulk materials and reduce the oxidation state of uranium.

2.2. Characterization

All samples were characterized for structure, phase purity, and composition. X-ray diffraction (XRD) was employed to identify the phases present, confirm the formation of a single phase, and determine the lattice parameter. A Bruker D-8 Advance diffractometer was used with Cu$K\alpha$ radiation and a rotating sample holder with operating parameters of 40 kV and 40 mA and a step size of 0.02° 2θ. The lattice parameter of each oxide sample was determined via whole pattern refinement by using Jade software.

Electron probe microanalysis (EPMA) with wavelength dispersive spectroscopy (WDS) was used to determine the composition and homogeneity of the samples. Pellets of 3.0 mm in diameter were prepared by sintering and then mounted and carefully polished to 1 μm surface roughness using SiC papers and then diamond paste. Chemical compositional analyses were performed on 10–15 random points of 1 μm size and averaged for each sample. The metal ratio of each sample was determined, but not the oxygen content, since the oxidation states of U are not fixed and EPMA can not determine oxygen content directly. The standards used were $LaPO_4$ for La (L_α line), $Y_3Al_5O_{12}$ for Y (L_α line), $NdPO_4$ for Nd (L_α line), and UO_2 for U (M_α line).

2.3. Titration for uranium oxidation state (oxygen content) determination

To obtain the complete composition of each rare earth doped uranium oxide sample, the oxidation state of U was determined by a Ce(IV)–Fe(II) back titration method after dissolving the rare-earth doped uranium oxide in a warm mixture of sulphuric and phosphoric acids containing excess Ce(IV) [20]. In order to oxidize the uranium exclusively by Ce(IV) in the acid mixture, nitrogen was bubbled through the solution for the whole process. In this method, all uranium in the solid was oxidized to U(VI):

$$U(IV) + 2Ce(IV) \rightarrow U(VI) + 2Ce(III) \quad (1)$$

The excess Ce(IV) was then back titrated with Fe(II) solution:

$$Ce(IV) + Fe(II) \rightarrow Ce(III) + Fe(III) \quad (2)$$

All the solutions used here were prepared with analytical reagent grade chemicals and de-ionized water. 0.05 mol/L of Ce(IV) solution was prepared by diluting standard 0.1 mol/L $Ce(SO_4)_2$ solution in 1.5 mol/L sulphuric acid, while 0.05 mol/L Fe(II) solution was prepared by dissolving certain amount of $FeSO_4\cdot(NH_4)SO_4\cdot 6H_2O$ in 1.5 mol/L sulphuric acid.

The various rare earth doped uranium oxide samples (20–30 mg) were weighed and transferred to a 50 ml titration flask by washing with deionized water. Then 5 ml of 0.05 mol/L Ce(IV) sulphate solution was added using a calibrated pipette, followed by 5 ml 1.5 mol/L sulphuric acid, and 1–1.5 ml concentrated phosphoric acid. The flask was then heated to about 80 °C with N_2 bubbling through the solution during the entire process in order to prevent oxidation by O_2 in the atmosphere. The oxides were dissolved completely in a few hours. After dissolution, several ml of sulphuric acid were added to dilute the solution. The solution was then back titrated by 0.05 mol/L Fe(II) solution to determine the remaining Ce(IV), thereby the amount of Ce(IV) used to oxidize U(IV) in the samples could be obtained by subtracting the remaining Ce(IV) from the added one before dissolution.

The back titration of the remaining Fe(II) was carried out in two ways, a manual mode and by a potentiometric autotitrator (Mettler Toledo T50). At first, the back titration was carried out manually. Several drops of ferroin indicator were added and the solution was titrated with 0.05 mol/L Fe(II) solution from a 10 ml burette with a precision of 0.025 ml. The endpoint was determined by observing the color change of the solution turning from blue to red. Later a procedure was developed using a potentiometric autotitrator. The solution after complete dissolution was transferred to the titration beaker by washing with 1.5 mol/L sulphuric acid. In this method, the end point was calculated after all the remaining Ce(IV) was reduced by Fe(II). Some of the samples were titrated using both procedures, which gave consistent results.

2.4. Calorimetry

A custom built Tian–Calvet high-temperature microcalorimeter was used to measure the enthalpies of solution in molten sodium molybdate ($3Na_2O{\cdot}4MoO_3$) at 703 °C, which allowed calculation of enthalpies of formation [21,22]. About 10 mg of sample was pressed into a small pellet 1.6 mm in diameter and then dropped from room temperature into a Pt crucible containing 20 g of molten oxide solvent in the calorimeter. The calorimetric assembly was flushed with oxygen at 70 mL/min and the molten solvent was bubbled with oxygen at 5 mL/min, in order to stir the melt to shorten the dissolution time and to provide an oxidizing atmosphere to oxidize all the uranium to the hexavalent state in the solvent. This methodology has been described previously and applied to a number of materials containing uranium [16,23]. The formation enthalpies of rare earth-doped uranium oxide materials were then obtained from calculation by thermodynamic cycles shown in Table 1. However, because of the addition of the parameter y, which represents the oxidation of uranium cations in the solid solutions, there are two ways to calculate the formation enthalpies of these oxides, form constituent oxides $LnO_{1.5}$ (Ln = La, Y, Nd), UO_2, and UO_3 or O_2, as shown in Table 1. Therefore, in this paper, we report two types of formation enthalpies for the samples, those with and without oxidation of the constituent oxides.

3. Results

Table 2 lists the chemical compositions obtained from electron microprobe analysis for the uranium and rare earth dopant concentration x, and by titration for the average uranium oxidation state z(U), and therefore the oxygen content, 2−0.5x + y, which is also the oxygen to metal O/M ratio. The oxygen content is then calculated by balancing the charges. All samples have O/M ratios larger than 2 except $La_{0.462}U_{0.538}O_{1.973}$, but their average oxidation state of U (z(U)) is mostly lower than 5+ (4 < z(U) < 5) both in Ln = La and Y systems, while Ln = Nd systems show higher average oxidation state, z(U) ≥ 5.0. Therefore we know that at least some part of uranium is hexavalent but we can not uniquely constrain how much is pentavalent. The titration methods can determine the average oxidation states of uranium in the doped oxides, but not quantify the amount of U^{4+}, U^{5+}, and U^{6+}, since a given average oxidation state between four and five can be satisfied by a mixture of U^{4+} and U^{5+}, of U^{4+} and U^{6+}, or an infinite number of combinations of U^{4+}, $U^{5+}$and U^{6+}. Nevertheless, to analyze the calorimetric data, calculate enthalpies of formation, and interpret the trends seen, it is sufficient to know the average oxidation state rather than detailed speciation. Indeed neither titrations nor thermodynamic measurements can distinguish specific oxidation states, though the average oxidation state inferred from these measurements is linked to the oxygen content.

All the samples showed only XRD peaks for a cubic fluorite phase. The lattice parameters given by the Rietveld refinement are listed in Table 2. The samples characterized by electron microprobe analysis show no secondary phases in back-scattered electron images and the compositions are consistent at different points in the sample. Thus the samples studied here are homogeneous single phases, at least within the spatial resolution of microprobe analysis, namely about 1 μm. Generally, when sintered at higher temperatures, the solid solutions get reduced to a higher degree in the 5% H_2/Ar atmosphere, hence a lower y value in the composition is obtained.

The calorimetric data are shown in Table 3, including enthalpies of drop solution and formation enthalpies from oxides or from oxides and oxygen at room temperature, calculated using the thermochemical cycles in Table 1. Previous experiments have shown that all uranium dissolved in molten sodium molybdate under these conditions is present entirely in the hexavalent state [24]. Therefore, for samples doped with a similar amount of rare earth cations, the ones with higher amounts of U^{6+} release less heat after being dropped into the solvent since less U^{4+} is oxidized to U^{6+} on dissolution.

For rare earth doped uranium oxide solid solutions formed from constituent oxides without oxidation, the formation reaction is:

$$xLnO_{1.5} + (1-x-y)\cdot UO_2 + yUO_3 \rightarrow Ln_xU_{1-x}O_{2-0.5x+y} \quad (3)$$

For all three dopants, the formation enthalpies ($\Delta H_{f,ox}$) become more negative as the dopant concentrations increase (see Fig. 1).

Table 1
Reactions and thermodynamic cycles used to calculate enthalpies of formation of the fluorite phase $Ln_xU_{1-x}O_{2-0.5x+y}$ at 25 °C from oxides with respect to A-type $LaO_{1.5}$ (C-type $YO_{1.5}$, or A-type $NdO_{1.5}$), UO_2 with fluorite structure, and UO_3 or oxygen.

Reaction	Enthalpy of the reaction (kJ/mol)
(1) $Ln_xU_{1-x}O_{2-0.5x+y}$ (fluorite 25 °C) + 0.5(1−x−y)O_2 (g, 703 °C) = x$LnO_{1.5}$ (soln, 703 °C) + (1−x)UO_3 (soln, 703 °C)	$\Delta H_{ds}^{(1)}$ ($Ln_xU_{1-x}O_{2-0.5x+y}$)
(2) $LnO_{1.5}$ (A-25 °C) = $LnO_{1.5}$ (soln, 703 °C)	$\Delta H_{ds}^{(2)}$ (A-$LaO_{1.5}$) = −112.5 ± 1.6 [37]
	$\Delta H_{ds}^{(2)}$ (C-$YO_{1.5}$) = −60.4 ± 0.9 [38]
	$\Delta H_{ds}^{(2)}$ (A-$NdO_{1.5}$) = −81.68 ± 1.72 [39]
(3) UO_2 (fluorite 25 °C) + 0.5O_2 (g, 703 °C) = UO_3 (soln, 703 °C)	$\Delta H_{ds}^{(3)}$ (UO_2) = −136.4 ± 2.3 [23]
(4) UO_3 (s, 25 °C) = UO_3 (soln, 703 °C)	$\Delta H_{ds}^{(4)}$ (UO_3) = 9.5 ± 1.5 [23]
(5) O_2 (g, 25 °C) = O_2 (g, 703 °C)	$\Delta H_{heat\ content}^{(5)}$ (O_2) = 21.8 [25]
(6) x$LnO_{1.5}$ (A/C-25 °C) + (1−x−y)UO_2 (fluorite 25 °C) + yUO_3 (25 °C) = $Ln_xU_{1-x}O_{2-0.5x+y}$ (fluorite 25 °C)	$\Delta H_{f,ox}^{(6)}$ ($Ln_xU_{1-x}O_{2-0.5x+y}$)
(7) x$LnO_{1.5}$ (A/C-25 °C) + (1−x)UO_2 (fluorite 25 °C) + 0.5yO_2 (g, 25 °C) = $Ln_xU_{1-x}O_{2-0.5x+y}$ (fluorite 25 °C)	$\Delta H_{f,ox+oxygen}^{(7)}$ ($Ln_xU_{1-x}O_{2-0.5x+y}$)
(8) Ln (s, 25 °C) + 0.5O_2 (g, 25 °C) = $LnO_{1.5}$ (s, 25 °C)	$\Delta H_{f,el}^{(8)}$ (A-$LaO_{1.5}$) = −897.1 ± 0.1 [40]
	$\Delta H_{f,el}^{(8)}$ (C-$YO_{1.5}$) = −952.5 ± 0.2 [40]
	$\Delta H_{f,el}^{(8)}$ (A-$NdO_{1.5}$) = −904.2 ± 0.2 [40]
(9) U (s, 25 °C) + O_2 (g, 25 °C) = UO_2 (fluorite, 25 °C)	$\Delta H_{f,el}^{(9)}$ (UO_2) = −1084.9 ± 1.0 [25]
(10) U (s, 25 °C) + 1.5O_2 (g, 25 °C) = UO_3 (s, 25 °C)	$\Delta H_{f,el}^{(10)}$ (UO_3) = −1223.8 [41]
(11) xLn (s, 25 °C) + (1−x)U (s, 25 °C) + 0.5*(2−0.5x + y)O_2 (g, 25 °C) = $Ln_xU_{1-x}O_{2-0.5x+y}$ (fluorite 25 °C)	$\Delta H_{f,el}^{(11)}$ ($Ln_xU_{1-x}O_{2-0.5x+y}$)

$\Delta H^{(6)} = -\Delta H^{(1)} + x\Delta H^{(2)} + (1-x-y)\Delta H^{(3)} + y\Delta H^{(4)}$.
$\Delta H^{(7)} = -\Delta H^{(1)} + x\Delta H^{(2)} + (1-x)\Delta H^{(3)} + 0.5y\Delta H^{(5)}$.
$\Delta H^{(11)} = \Delta H^{(6)} + x\Delta H^{(8)} + (1-x-y)\Delta H^{(9)} + y\Delta H^{(10)}$.

Table 2
Composition and lattice parameters of $Ln_xU_{1-x}O_{2-0.5x+y}$ solid solutions.

x	y	Average U oxidation state z(U)	Sintering condition (temperature/time)	Lattice parameter (Å)	Composition
$La_xU_{1-x}O_{2-0.5x+y}$					
0.100 ± 0.002	0.058 ± 0.02	4.13	1450 °C/24 h	5.4735	$La_{0.100}U_{0.900}O_{2.008}$ or $(LaO_{1.5})_{0.100}(UO_2)_{0.842}(UO_3)_{0.058}$
0.094 ± 0.003	0.120 ± 0.02	4.26	1350 °C/24 h	5.4773	$La_{0.094}U_{0.906}O_{2.073}$ or $(LaO_{1.5})_{0.094}(UO_2)_{0.786}(UO_3)_{0.120}$
0.206 ± 0.010	0.261 ± 0.02	4.66	1450 °C/24 h	5.4861	$La_{0.206}U_{0.794}O_{2.158}$ or $(LaO_{1.5})_{0.206}(UO_2)_{0.533}(UO_3)_{0.261}$
0.195 ± 0.009	0.457 ± 0.02	5.14	1350 °C/36 h	5.4780	$La_{0.195}U_{0.805}O_{2.3595}$ or $(LaO_{1.5})_{0.195}(UO_2)_{0.348}(UO_3)_{0.457}$
0.303 ± 0.040	0.262 ± 0.02	4.75	1450 °C/24 h	5.4963	$La_{0.303}U_{0.697}O_{2.1105}$ or $(LaO_{1.5})_{0.303}(UO_2)_{0.435}(UO_3)_{0.262}$
0.309 ± 0.025	0.337 ± 0.02	4.98	1350 °C/24 h	5.4918	$La_{0.309}U_{0.691}O_{2.1825}$ or $(LaO_{1.5})_{0.309}(UO_2)_{0.354}(UO_3)_{0.337}$
0.310 ± 0.048	0.374 ± 0.02	5.08	1250 °C/24 h	5.4993	$La_{0.310}U_{0.690}O_{2.219}$ or $(LaO_{1.5})_{0.310}(UO_2)_{0.316}(UO_3)_{0.374}$
0.462 ± 0.056	0.204 ± 0.02	4.76	1450 °C/24 h	5.5267	$La_{0.462}U_{0.538}O_{1.973}$ or $(LaO_{1.5})_{0.462}(UO_2)_{0.334}(UO_3)_{0.204}$
0.465 ± 0.065	0.348 ± 0.02	5.30	1300 °C/24 h	5.5280	$La_{0.465}U_{0.535}O_{2.1155}$ or $(LaO_{1.5})_{0.465}(UO_2)_{0.187}(UO_3)_{0.348}$
0.462 ± 0.056	0.340 ± 0.02	5.26	1100 °C/24 h	5.5292	$La_{0.462}U_{0.538}O_{2.109}$ or $(LaO_{1.5})_{0.462}(UO_2)_{0.198}(UO_3)_{0.340}$
$Y_xU_{1-x}O_{2-0.5x+y}$					
0.194 ± 0.007	0.312 ± 0.02	4.77	1450 °C/24 h	5.4029	$Y_{0.194}U_{0.806}O_{2.215}$ or $(YO_{1.5})_{0.194}(UO_2)_{0.494}(UO_3)_{0.312}$
0.183 ± 0.012	0.409 ± 0.02	5.00	1350 °C/36 h	5.4010	$Y_{0.183}U_{0.817}O_{2.3175}$ or $(YO_{1.5})_{0.183}(UO_2)_{0.408}(UO_3)_{0.409}$
0.328 ± 0.034	0.230 ± 0.02	4.68	1350 °C/24 h	5.3822	$Y_{0.328}U_{0.672}O_{2.066}$ or $(YO_{1.5})_{0.328}(UO_2)_{0.442}(UO_3)_{0.230}$
0.315 ± 0.038	0.190 ± 0.02	4.55	1250 °C/24 h	5.3889	$Y_{0.315}U_{0.685}O_{2.0325}$ or $(YO_{1.5})_{0.315}(UO_2)_{0.495}(UO_3)_{0.190}$
0.455 ± 0.010	0.240 ± 0.02	4.88	1450 °C/24 h	5.3532	$Y_{0.455}U_{0.545}O_{2.0125}$ or $(YO_{1.5})_{0.455}(UO_2)_{0.305}(UO_3)_{0.240}$
0.471 ± 0.017	0.254 ± 0.02	4.96	1350 °C/36 h	5.3471	$Y_{0.471}U_{0.529}O_{2.0185}$ or $(YO_{1.5})_{0.471}(UO_2)_{0.275}(UO_3)_{0.254}$
0.472 ± 0.009	0.274 ± 0.02	5.04	1250 °C/36 h	5.3510	$Y_{0.472}U_{0.528}O_{2.038}$ or $(YO_{1.5})_{0.472}(UO_2)_{0.254}(UO_3)_{0.312}$
$Nd_xU_{1-x}O_{2-0.5x+y}$					
0.196 ± 0.022	0.383 ± 0.02	4.95	1450 °C/24 h	5.4463	$Nd_{0.196}U_{0.804}O_{2.285}$ or $(NdO_{1.5})_{0.196}(UO_2)_{0.421}(UO_3)_{0.383}$
0.201 ± 0.018	0.402 ± 0.02	5.01	1350 °C/36 h	5.4460	$Nd_{0.201}U_{0.799}O_{2.3015}$ or $(NdO_{1.5})_{0.201}(UO_2)_{0.397}(UO_3)_{0.402}$
0.297 ± 0.017	0.254 ± 0.02	4.72	1450 °C/24 h	5.4517	$Nd_{0.297}U_{0.703}O_{2.1055}$ or $(NdO_{1.5})_{0.297}(UO_2)_{0.449}(UO_3)_{0.254}$
0.315 ± 0.013	0.350 ± 0.02	5.02	1350 °C/36 h	5.4504	$Nd_{0.315}U_{0.685}O_{2.1925}$ or $(NdO_{1.5})_{0.315}(UO_2)_{0.335}(UO_3)_{0.350}$
0.507 ± 0.024	0.255 ± 0.02	5.03	1450 °C/24 h	5.4519	$Nd_{0.507}U_{0.493}O_{2.0015}$ or $(NdO_{1.5})_{0.507}(UO_2)_{0.238}(UO_3)_{0.255}$
0.502 ± 0.023	0.302 ± 0.02	5.21	1350 °C/36 h	5.4511	$Nd_{0.502}U_{0.498}O_{2.051}$ or $(NdO_{1.5})_{0.502}(UO_2)_{0.196}(UO_3)_{0.302}$
0.507 ± 0.029	0.306 ± 0.02	5.24	1250 °C/36 h	5.4491	$Nd_{0.507}U_{0.493}O_{2.0525}$ or $(NdO_{1.5})_{0.507}(UO_2)_{0.187}(UO_3)_{0.306}$

Samples with the same dopant concentration exhibit similar formation enthalpies despite different uranium oxidation states for all three groups of rare earth doped uranium oxides.

The formation enthalpies at room temperature of the solid solutions from $LnO_{1.5}$, UO_2 and O_2, thus involving oxidation, are also listed in Table 3. These enthalpies ($\Delta H_{f,ox+oxygen}$) refer to the reaction:

$$xLnO_{1.5} + (1-x)\cdot UO_2 + 0.5yO_2 \rightarrow Ln_xU_{1-x}O_{2-0.5x+y} \quad (4)$$

The formation enthalpies for this reaction are much more negative than the ones from constituent oxides, Ln_2O_3, UO_2 and UO_3, simply because the oxidation reaction of UO_2 to UO_3 is very exothermic [25].

While Mazeina et al. [16] presented initial calorimetric data on Ca- and Y-doped uranium oxides, the energetics of the system have not been explored over the whole range and the oxygen content of the samples was not determined accurately. For instance, they reported one sample, $Y_{0.32}U_{0.68}O_{2.13}$ with an enthalpy of drop solution of −55.3 ± 1.2 kJ/mol, which is between the two $Y_{0.32}U_{0.68}O_{2-0.5x+y}$ samples in this paper (see Table 3), −50.99 ± 1.35 kJ/mol and −57.84 ± 1.91 kJ/mol. Thus the oxygen content of that sample may be between that of these two samples despite the slight differences in x between the samples. However, its oxygen content was reported to be 2.13, which is much higher than our samples, 2.066 and 2.033. Because of this possibly inaccurate determination of chemical composition, their calculated formation enthalpy from constituent oxides (UO_2, UO_3, and $YO_{1.5}$) is −14.5 ± 3.2 kJ/mol, which is less negative than our values, −26.92 ± 1.75 kJ/mol and −26.90 ± 2.26 kJ/mol. If we assume the $\Delta H_{f,ox}$ of this sample is similar to the samples reported here, as observed in all doped uranium oxides, then we can calculate its composition to be $Y_{0.32}U_{0.68}O_{2.045}$ instead of $Y_{0.32}U_{0.68}O_{2.13}$. The drop solution enthalpy of this $Y_{0.32}U_{0.68}O_{2.045}$ sample is −246 ± 5 J/g and −55.0 ± 1.2 kJ/mol. Using the corrected composition and drop solution enthalpy of the $Y_{0.32}U_{0.68}O_{2.045}$ sample, we can calculate its $\Delta H_{f,ox}$ and $\Delta H_{f,ox+oxygen}$ to be −27.17 ± 1.68 kJ/mol and −54.85 ± 1.99 kJ/mol, which are consistent with our reported data here. Despite some possible uncertainties, Mazeina et al. also found the formation enthalpies of the Y-doped uranium oxides to become more exothermic with increasing dopant concentration, which is consistent with our findings.

The enthalpies of formation of the rare earth doped uranium oxides from elements at room temperature are expressed by the reaction,

$$xLn + (1-x)\cdot U + 0.5^*(2-0.5x+y)\cdot O_2 \rightarrow Ln_xU_{1-x}O_{2-0.5x+y} \quad (5)$$

Their values are calculated based on the thermochemical cycles shown in Table 1, and listed in Table 4.

4. Discussion

4.1. Lattice parameters

When sintered under different conditions, uranium oxide doped with similar amounts of rare earth cations oxidizes to a different extent, resulting in different oxygen content in the solid solution. The resulting lattice parameters are slightly different as well, as shown in Fig. 2. Because both rare earth content and oxygen content vary, and both affect the lattice parameters, Vegard's Law is not strictly followed. With increasing dopant concentration, the lattice parameters of the La-doped uranium oxides increase, those of the Y-doped solid solutions decrease, while the ones of the Nd-doped system change very little if at all. At first glance, the trends seem inconsistent with the ionic radii of La^{3+} (1.16 Å), Y^{3+} (1.02 Å), Nd^{3+} (1.11 Å), and U^{4+} (1.00 Å) in eight-fold coordination [26], which would predict significant increase in lattice parameter for La and Nd but little change for Y if cation size difference were the dominant factor.

However, the lattice parameter changes are caused not only by the cation radius difference, but also the anion defect formation.

Table 3
Enthalpies of drop solution (into sodium molybdate, $3Na_2O{\cdot}4MoO_3$) at 703 °C, and enthalpies of formation of $Ln_xU_{1-x}O_{2-0.5x+y}$ solid solutions with respect to A-type $LaO_{1.5}$ (C-type $YO_{1.5}$, or A-type $NdO_{1.5}$), UO_2 with fluorite structure, and oxygen.

Composition	Enthalpy of drop solution $\Delta H_{ds}^{(1)}$	$\Delta H_{f,ox}^{(6)}$	$\Delta H_{f,ox+oxygen}^{(7)}$
$La_{0.100}U_{0.900}O_{2.008}$	−116.36 ± 1.06	−9.19 ± 2.21	−17.02 ± 2.33
$La_{0.094}U_{0.906}O_{2.073}$	−107.54 ± 1.20	−9.11 ± 2.18	−25.31 ± 2.41
$La_{0.206}U_{0.794}O_{2.158}$	−72.64 ± 0.64	−20.62 ± 1.47	−55.99 ± 1.96
$La_{0.195}U_{0.805}O_{2.3595}$	−41.57 ± 1.14	−23.49 ± 1.58	−85.19 ± 2.20
$La_{0.303}U_{0.697}O_{2.1105}$	−48.60 ± 2.75	−42.33 ± 2.99	−77.70 ± 3.22
$La_{0.309}U_{0.691}O_{2.1825}$	−35.14 ± 2.64	−44.70 ± 2.85	−90.20 ± 3.12
$La_{0.310}U_{0.690}O_{2.219}$	−29.26 ± 1.39	−45.16 ± 1.74	−95.65 ± 2.17
$La_{0.462}U_{0.538}O_{1.973}$	−44.28 ± 1.92	−51.32 ± 2.21	−78.86 ± 2.40
$La_{0.465}U_{0.535}O_{2.1155}$	−22.66 ± 1.43	−51.86 ± 1.75	−98.84 ± 2.03
$La_{0.462}U_{0.538}O_{2.109}$	−21.34 ± 0.29	−54.41 ± 1.08	−100.31 ± 1.49
$Y_{0.194}U_{0.806}O_{2.215}$	−57.42 ± 1.44	−18.72 ± 1.90	−60.84 ± 2.36
$Y_{0.183}U_{0.817}O_{2.3175}$	−43.74 ± 1.88	−19.07 ± 2.19	−74.29 ± 2.66
$Y_{0.328}U_{0.672}O_{2.066}$	−50.99 ± 1.35	−26.92 ± 1.75	−57.97 ± 2.07
$Y_{0.315}U_{0.685}O_{2.0325}$	−57.84 ± 1.91	−26.90 ± 2.26	−52.55 ± 2.49
$Y_{0.455}U_{0.545}O_{2.0125}$	−23.97 ± 0.79	−42.83 ± 1.19	−75.23 ± 1.54
$Y_{0.471}U_{0.529}O_{2.0185}$	−18.44 ± 0.65	−45.10 ± 1.07	−79.39 ± 1.44
$Y_{0.472}U_{0.528}O_{2.038}$	−17.20 ± 0.65	−43.35 ± 1.06	−80.34 ± 1.44
$Nd_{0.196}U_{0.804}O_{2.285}$	−42.96 ± 0.53	−27.27 ± 1.29	−78.57 ± 1.95
$Nd_{0.201}U_{0.799}O_{2.3015}$	−37.61 ± 0.97	−28.12 ± 1.50	−83.33 ± 2.11
$Nd_{0.297}U_{0.703}O_{2.1055}$	−49.08 ± 1.10	−34.01 ± 1.64	−68.30 ± 2.02
$Nd_{0.315}U_{0.685}O_{2.1925}$	−30.46 ± 0.54	−37.93 ± 1.21	−84.91 ± 1.75
$Nd_{0.507}U_{0.493}O_{2.0015}$	−18.05 ± 0.73	−52.82 ± 1.32	−87.78 ± 1.61
$Nd_{0.502}U_{0.498}O_{2.051}$	−13.92 ± 0.92	−51.24 ± 1.41	−91.74 ± 1.70
$Nd_{0.507}U_{0.493}O_{2.0525}$	−12.99 ± 0.76	−51.75 ± 1.32	−92.39 ± 1.62

All data are in kJ/mol.

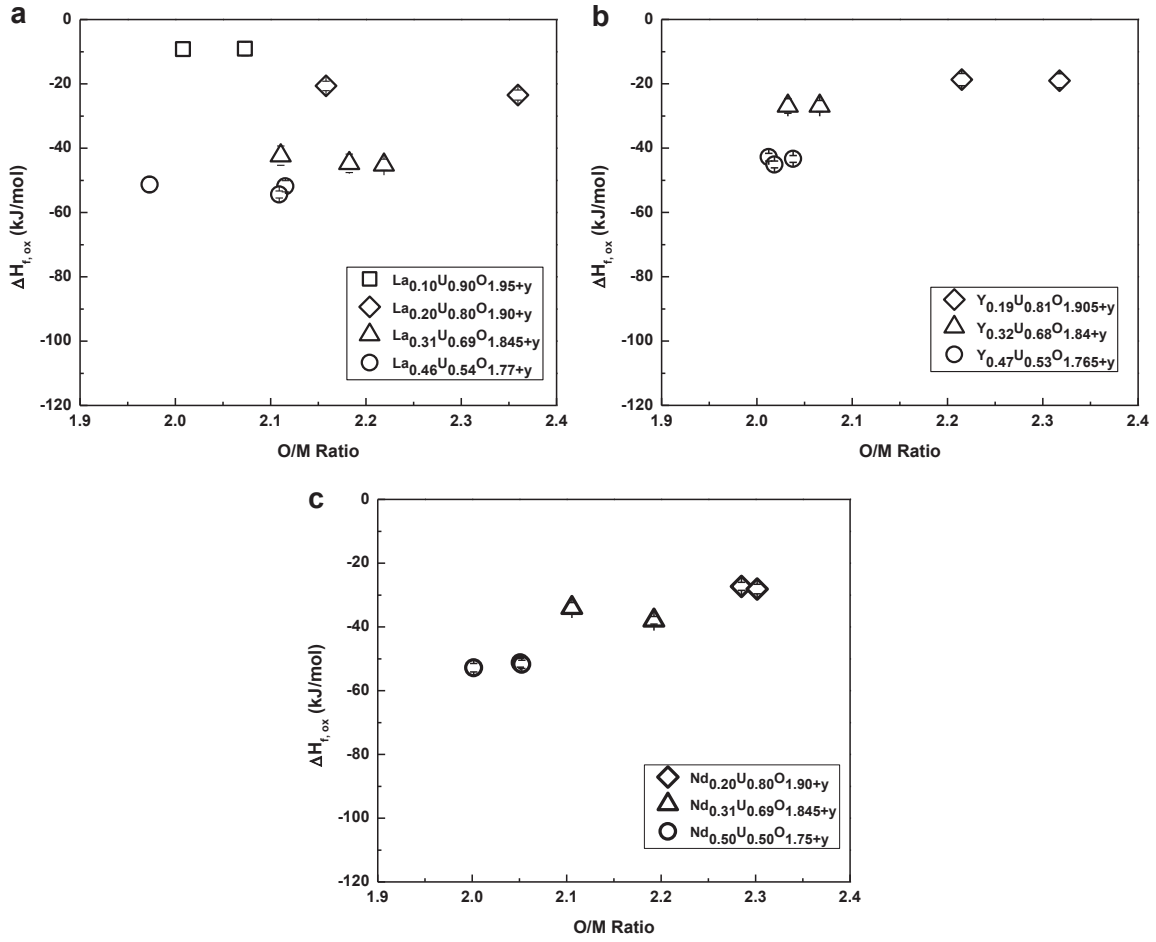

Fig. 1. Enthalpies of formation of $Ln_xU_{1-x}O_{2-0.5x+y}$ solid solutions from A-type $LaO_{1.5}$ (C-type $YO_{1.5}$ or A-type $NdO_{1.5}$), fluorite UO_2 and UO_3, as a function of O/M ratio, with various dopant concentrations.

Kim has summarized the empirical equations for the lattice parameter changes of doped HfO_2, ZrO_2, CeO_2, and ThO_2 solid solutions, and then estimated the one for doped UO_2 solution [27]. From these equations, a critical ionic radius of aliovalent dopant into fluorite structured oxides can be determined, which is the radius for which substitution causes neither expansion nor contraction. The critical ionic radius for a trivalent dopant into UO_2, is estimated to be 1.06 Å [27]. This is in good agreement with the observation in this paper that the Y-doped uranium oxides have decreasing lattice parameters with dopant concentrations despite the larger cation radius of Y^{3+} than of U^{4+}. Based on the experimental data, this critical ionic radius for substitution into UO_2 is very close to the ionic radius of Nd^{3+}, 1.109 Å, which is moderately close to the estimate made by Kim, 1.06 Å [27]. In addition, the lattice parameters of the three different rare earth doped uranium oxides extrapolate to about 5.45 Å when dopant concentration goes to zero, which is slightly smaller than that of stoichiometric UO_2, 5.47 Å [28]. This extrapolated lattice parameter of the oxides is correlated to $UO_{2.18}$ [29], thereby also supporting that some U^{6+} is present in our samples, reflecting its smaller ionic radius [26].

4.2. Enthalpies of formation $\Delta H_{f,ox}$ and $\Delta H_{f,ox+oxygen}$

The formation enthalpies at room temperature of the La-, Y-, and Nd-doped uranium oxide systems from A-type $LaO_{1.5}$, C-type $YO_{1.5}$, or A-type $NdO_{1.5}$ fluorite UO_2 and O_2, $\Delta H_{f,ox+oxygen}$, as a function of oxygen to metal (O/M) ratio, where $O/M = 2-0.5x+y$, are shown in Fig. 3. Comparing the formation enthalpies of solid solutions with similar rare earth dopant concentrations but different uranium oxidation states constrains the enthalpy of the oxidation reaction for $Ln_xU_{1-x}O_{2-0.5x+y}$,

$$Ln_xU_{1-x}O_{2-0.5x+y} + 0.5\delta y O_2 \rightarrow Ln_xU_{1-x}O_{2-0.5x+(y+\delta y)} \quad (6)$$

As shown in Fig. 3, the slopes of the lines correspond to the oxidation enthalpies of these oxides and are very similar despite different dopant concentrations and oxygen contents (see Table 5). Most of the slopes give values similar to the oxidation enthalpy of UO_2 at room temperature (Eq. (7)),

Table 4
Enthalpies of formation of $Ln_xU_{1-x}O_{2-0.5x+y}$ solid solutions from elements at room temperatures (298 K).

Composition	$\Delta H_{f,el}^{(11)}$ (kJ/mol)	$\Delta H_{f,el}$ (kJ/mol)	Difference (%)
$La_{0.100}U_{0.900}O_{2.008}$	−1083.37 ± 2.36	−1084.56 ± 0.95	0.11
$La_{0.094}U_{0.906}O_{2.073}$	−1093.02 ± 2.32	−1093.67 ± 0.88	0.06
$La_{0.206}U_{0.794}O_{2.158}$	−1103.09 ± 1.56	−1103.85 ± 1.03	0.07
$La_{0.195}U_{0.805}O_{2.3595}$	−1135.25 ± 1.62	−1132.00 ± 0.91	0.29
$La_{0.303}U_{0.697}O_{2.1105}$	−1106.72 ± 3.02	−1095.84 ± 1.37	0.98
$La_{0.309}U_{0.691}O_{2.1825}$	−1118.38 ± 2.87	−1105.75 ± 1.38	1.13
$La_{0.310}U_{0.690}O_{2.219}$	−1123.79 ± 1.77	−1110.81 ± 1.37	1.16
$La_{0.462}U_{0.538}O_{1.973}$	−1077.79 ± 2.24	−1074.43 ± 2.02	0.31
$La_{0.465}U_{0.535}O_{2.1155}$	−1097.77 ± 1.76	−1094.18 ± 2.01	0.33
$La_{0.462}U_{0.538}O_{2.109}$	−1099.77 ± 1.10	−1093.32 ± 2.00	0.59
$Y_{0.194}U_{0.806}O_{2.215}$	−1121.27 ± 1.96	−1122.69 ± 0.97	0.13
$Y_{0.183}U_{0.817}O_{2.3175}$	−1136.55 ± 2.23	−1136.48 ± 0.89	0.01
$Y_{0.328}U_{0.672}O_{2.066}$	−1100.34 ± 1.81	−1107.47 ± 1.48	0.65
$Y_{0.315}U_{0.685}O_{2.0325}$	−1096.49 ± 2.31	−1102.28 ± 1.44	0.53
$Y_{0.455}U_{0.545}O_{2.0125}$	−1100.82 ± 1.23	−1105.22 ± 1.98	0.40
$Y_{0.471}U_{0.529}O_{2.0185}$	−1102.92 ± 1.11	−1106.71 ± 2.05	0.34
$Y_{0.472}U_{0.528}O_{2.038}$	−1103.82 ± 1.09	−1109.46 ± 2.05	0.51
$Nd_{0.196}U_{0.804}O_{2.285}$	−1129.95 ± 1.36	−1123.03 ± 0.94	0.61
$Nd_{0.201}U_{0.799}O_{2.3015}$	−1132.54 ± 1.55	−1125.28 ± 0.95	0.64
$Nd_{0.297}U_{0.703}O_{2.1055}$	−1100.52 ± 1.71	−1097.34 ± 1.36	0.29
$Nd_{0.315}U_{0.685}O_{2.1925}$	−1114.52 ± 1.26	−1109.29 ± 1.40	0.47
$Nd_{0.507}U_{0.493}O_{2.0015}$	−1081.52 ± 1.35	−1081.33 ± 2.20	0.02
$Nd_{0.502}U_{0.498}O_{2.051}$	−1087.38 ± 1.43	−1088.24 ± 2.17	0.08
$Nd_{0.507}U_{0.493}O_{2.0525}$	−1087.54 ± 1.34	−1088.42 ± 2.19	0.08

$$UO_2 + 0.5O_2 \rightarrow UO_3 \quad (7)$$

which is very exothermic, $\Delta H = -138.9 \pm 1.3$ kJ/mol [25].

The large uncertainty in the $Y_{0.47}U_{0.53}O_{1.765+y}$ oxidation enthalpy is likely the result of the very close y values and relatively big differences of the dopant concentration (arising from the relatively large uncertainty in Δx as shown in Table 2). In addition, the bigger discrepancies in the Nd-doped system may arise from the large difference in the dopant cation concentration coupled with the small difference in the oxidation states of uranium, which makes the slope more uncertain. Despite these uncertainties, it appears that the enthalpy of oxidation of uranium in all these solid solutions is very similar to that of the oxidation of UO_2 to UO_3. In a previous paper [16], Mazeina et al. assumed that the energetics of oxidation of UO_2 can be approximately applied for the enthalpies of oxidation in the solid solutions, since similar observations had been found in the oxidation of iron, manganese and cobalt in spinels [30,31] and of copper in Sr and Ba doped La_2CuO_4 [32]. They argued that this oxidation is so exothermic that the introduction of rare earth dopants would only perturb it to a small extent. Our results support this conjecture. The present study supports such arguments and the similarity in enthalpy of oxidation perhaps suggests that the oxidized uranium is energetically similar to that in the hexavalent state, even for average oxidation state less than 5+. Nevertheless thermochemical and analytical data provide only the average oxidation state and can not distinguish whether the actual oxidation state is 5+, 6+, or a mixture of both.

The majority of the samples prepared in this work have oxygen content larger than 2. Therefore, the substitution of rare earth cations into the host fluorite structure is compensated by the oxidation of uranium cations and introduction of oxygen interstitials, as shown in Eq. (8),

$$xLnO_{1.5} + yU_U^x + \frac{1}{2}yO_2 \xrightarrow{UO_2} xLn'_U + yU_U^{\cdot} + 2xO_O^X + \left(y - \frac{1}{2}x\right)O_i'' \quad (8)$$

In contrast for solid solutions with oxygen contents smaller than 2, the lanthanide substitution is accommodated by oxygen vacancies,

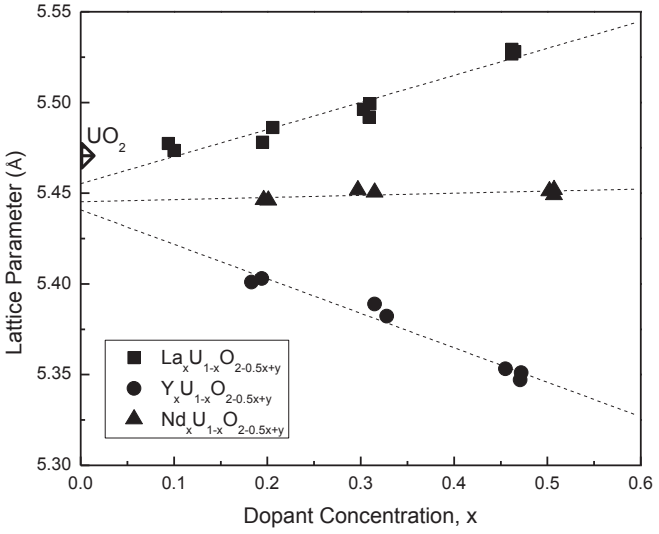

Fig. 2. Lattice parameters of the $Ln_xU_{1-x}O_{2-0.5x+y}$ solid solutions shown as a function of rare-earth dopant concentration, with various uranium oxidation states for samples with similar dopant concentrations.

$$xLnO_{1.5} + yU_U^x + \frac{1}{2}yO_2 \xrightarrow{UO_2} xLn'_U + yU_U^{\cdot\cdot} + \left(\frac{3}{2}x + y\right)O_O^X + \left(\frac{1}{2}x - y\right)V_O^{\cdot\cdot} \quad (9)$$

It is likely that different energetics control the oxidation behavior of the rare earth doped uranium oxides with different dominant oxygen defects in the substitution mechanism, and conclusions for the oxygen excess (interstitial) region can not be extrapolated to the oxygen deficiency (vacancy) region. Because we mainly have experimental data on the oxygen interstitial region, we conclude that the observation of the similarity between the oxidation enthalpy of the materials of interest in this paper and UO_2, as well as the lack of dependence on oxidation state of the formation enthalpies of these materials from UO_2, UO_3, and $LnO_{1.5}$ is so far validated only in the oxygen excess region.

Based on the above arguments, we can estimate the formation enthalpies of the rare earth doped uranium oxides $Ln_xU_{1-x}O_2$ from oxides down to oxygen content equal to 2, representing the phase with a stoichiometric oxygen sublattice with negligible concentration of vacancies or interstitials (Eq. (10)),

$$xLnO_{1.5} + (1-1.5x)UO_2 + 0.5xUO_3 \rightarrow Ln_xU_{1-x}O_2 \quad (10)$$

The results are shown in Fig. 4. The three rare earth doped oxides show a significantly more exothermic reaction when dopant content increases. Despite the La system being slightly more exothermic than the Y and Nd systems, the formation enthalpies of all three $Ln_xU_{1-x}O_2$ oxides seem to fit a linear relation between enthalpy of formation and dopant content with a slope of -103.8 ± 4.3 kJ/mol for all three dopants. Thus we can approximate the formation enthalpies of $Ln_xU_{1-x}O_2$ from oxides (when $O/M \geq 2$) as:

$$\Delta H_{f,\,ox} = -(103.8 \pm 4.3)x \ \text{(kJ/mol)} \quad (11)$$

Table 5
Oxidation enthalpies of $Ln_xU_{1-x}O_{2-0.5x+y}$ solid solutions at room temperature.

Composition	Oxidation enthalpy (kJ/mol)[a]
$La_{0.10}U_{0.90}O_{1.95+y}$	−134
$La_{0.20}U_{0.80}O_{1.90+y}$	−150
$La_{0.31}U_{0.69}O_{1.845+y}$	−160 ± 4
$La_{0.46}U_{0.54}O_{1.77+y}$	−149 ± 20
$Y_{0.19}U_{0.81}O_{1.905+y}$	−139
$Y_{0.32}U_{0.68}O_{1.84+y}$	−136
$Y_{0.47}U_{0.53}O_{1.765+y}$	−140 ± 70
$Nd_{0.20}U_{0.80}O_{1.90+y}$	−250
$Nd_{0.31}U_{0.69}O_{1.845+y}$	−172
$Nd_{0.50}U_{0.50}O_{1.75+y}$	−88 ± 5
UO_2	−138.9 ± 1.3 [25]

[a] No error is reported when the oxidation enthalpy is obtained from only two samples with similar dopant concentration but different oxidation states.

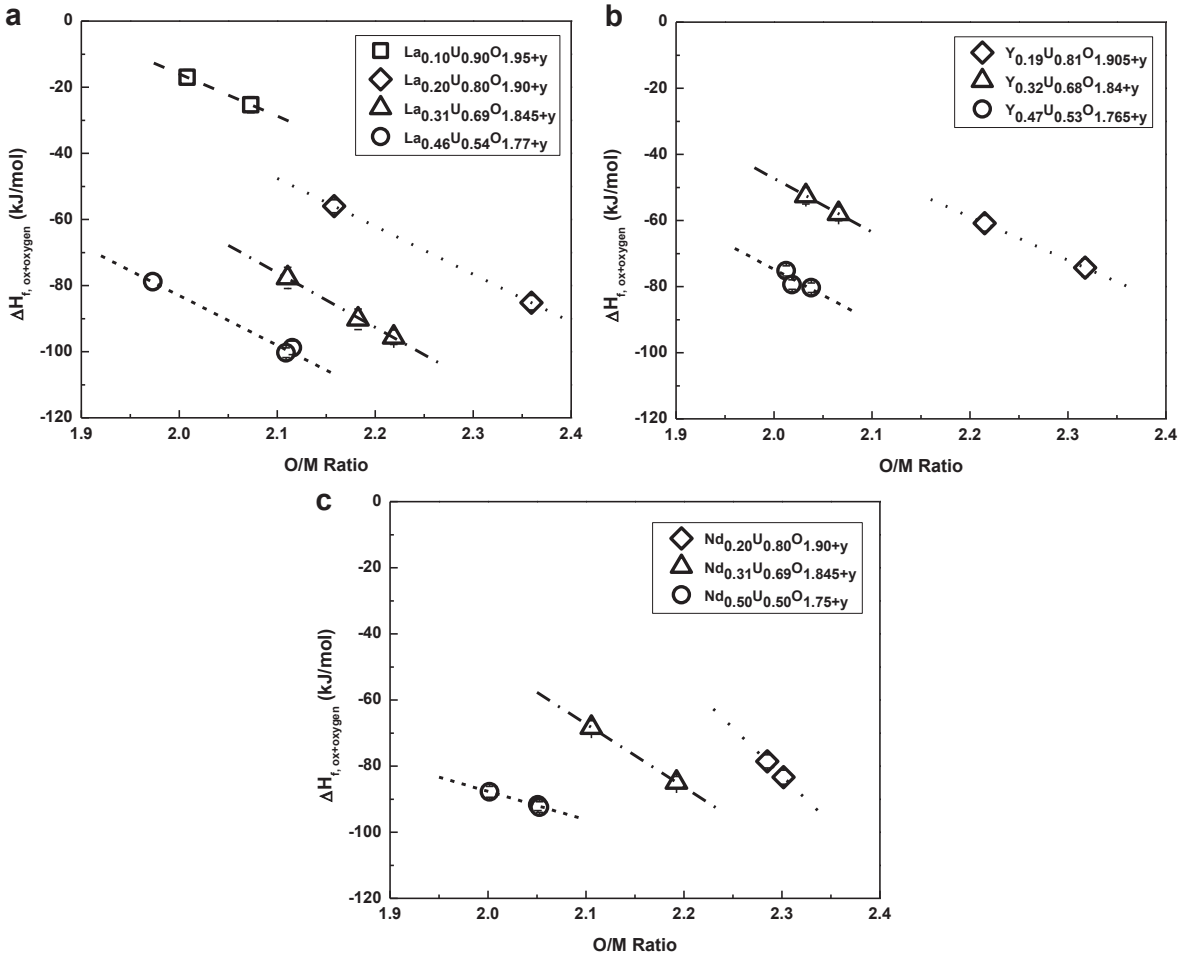

Fig. 3. Enthalpies of formation of $Ln_xU_{1-x}O_{2-0.5x+y}$ solid solutions from A-type $LaO_{1.5}$ (C-type $YO_{1.5}$ or A-type $NdO_{1.5}$), fluorite UO_2 and O_2, as a function of O/M ratio, with various dopant concentrations.

4.3. Enthalpies of formation from elements $\Delta H_{f,el}$

Using Eq. (11), we can approximate the formation enthalpies of $Ln_xU_{1-x}O_{2-0.5x+y}$ from elements at room temperature as:

$$\Delta H_{f,el} = \Delta H_{f,ox} + x\Delta H^{(8)}_{f,el}(LnO_{1.5}) + (1-x-y)\Delta H^{(9)}_{f,el}(UO_2) + y\Delta H^{(10)}_{f,el}(UO_3) \quad (12)$$

The equations thus obtained for $Ln_xU_{1-x}O_{2-0.5x+y}$ (Ln = La, Y, Nd) are listed in Table 6. $\Delta H_{f,el}$ of $Ln_xU_{1-x}O_{2-0.5x+y}$ samples are calculated using the fit equations in Table 6 and are listed in Table 4 and are compared with their $\Delta H^{(6)}_{f,el}$ values from calorimetric measurements. The differences between the calculated and measured values are generally within 1% over a wide range of dopant concentrations and oxygen contents.

With the above calculation of $\Delta H_{f,el}$ at room temperature, a direct comparison of the enthalpy data from calorimetric measurements and those derived from free energy measurements becomes possible, even though the latter refer to compositions different from those used in the calorimetric measurements. We calculate the formation free energies of $Ln_xU_{1-x}O_{2-0.5x+y}$ at different temperatures:

$$\Delta G_{f,el} = x\Delta G_{f,el}(LnO_{1.5}) + (1-x)\Delta G_{f,el}(UO_2) + \frac{y}{2}\Delta\overline{G}_{O_2} \quad (13)$$

where $\Delta G_{f,el}(LnO_{1.5})$ and $\Delta G_{f,el}(UO_2)$ are taken from Ref. [33], and

$$\Delta\overline{G}_{O_2} = RTlnp_{O_2} \quad (14)$$

The calculated $\Delta G_{f,el}(Ln_xU_{1-x}O_{2-0.5x+y})$ values are fitted linearly by Eq. (15) in the reported temperature ranges.

$$\Delta G_{f,el} = A + BT \quad (15)$$

with coefficients A and −B representing the enthalpy of formation $\Delta H_{f,el,T}$ $(Ln_xU_{1-x}O_{2-0.5x+y})$ and entropy of formation $\Delta S_{f,el,T}$ $(Ln_xU_{1-x}O_{2-0.5x+y})$, approximated to be constant over the measured temperature range.

$\Delta H_{f,el,T}$ and $\Delta S_{f,el,T}$ of a few samples ($La_{0.025}U_{0.975}O_{2.075}$, $La_{0.05}U_{0.95}O_{2.01}$, $La_{0.05}U_{0.95}O_{2.10}$, $La_{0.2}U_{0.8}O_2$, $Y_{0.025}U_{0.975}O_{2.05}$, $Y_{0.025}U_{0.975}O_{2.20}$, and $Y_{0.048}U_{0.952}O_{2.125}$) with different dopants, dopant concentrations and oxygen contents are calculated from Refs. [12,15] using the above methods and are listed in Table 7, along with their $\Delta H_{f,el}$ values at 298 K obtained using equations from Table 6. In order to compare the measured and calculated formation enthalpies, the differences between the high temperature $\Delta H_{f,el,T}$ and the room temperature $\Delta H_{f,el,298\ K}$, are calculated by:

$$\Delta H_{f,el,T} - \Delta H_{f,el,298\ K} = \int_{298\ K}^{T} \Delta C_p dT \quad (16)$$

where C_p of the elements are taken from Ref. [33]. Using the heat capacity measurements of lanthanum doped uranium oxides with different $LaO_{1.5}$ contents from Ref. [34], $\int_{298\ K}^{T} \Delta C_p dT$ values are calculated to be less than −8 kJ/mol at 1173–1573 K for the reported compositions, thus $\Delta H_{f,el,T}$ can be compared with $\Delta H_{f,el,298\ K}$ directly. As shown in Table 7, they are consistent with each other within 2%. The good agreement validates both the calorimetric and free energy data and suggests that our method for interpolating enthalpies of formation for different compositions is robust.

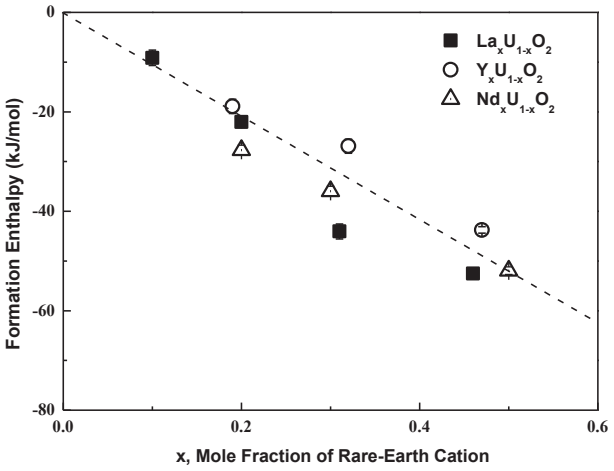

Fig. 4. Enthalpies of formation of $Ln_xU_{1-x}O_2$ solid solutions estimated from A-type $LaO_{1.5}$ (C-type $YO_{1.5}$ or A-type $NdO_{1.5}$), fluorite UO_2 and UO_3, as a function of rare-earth dopant concentration, x.

4.4. Enthalpies and entropies of formation from oxides $\Delta H_{f,ox}$ and $\Delta S_{f,ox}$

The formation enthalpies and entropies from oxides, $\Delta H_{f,ox}$ and $\Delta S_{f,ox}$ of the doped uranium oxides listed in Table 7, can be calculated by

$$\Delta H_{f,ox} = \Delta H_{f,el} - \frac{x}{2}\Delta H_{f,el}(Ln_2O_3) - (1-x-y)\Delta H_{f,el}(UO_2) - y\Delta H_{f,el}(UO_3) \quad (17)$$

$$\Delta S_{f,ox} = \Delta S_{f,el} - \frac{x}{2}S^o(Ln_2O_3) - (1-x-y)S^o(UO_2) - yS^o(UO_3) + xS^o(La) + (1-x)S^o(U) + \frac{2-0.5x+y}{2}S^o(O_2) \quad (18)$$

Since UO_3 decomposes to U_3O_8 above 900 K [35], we aim to get the $\Delta H_{f,ox}$ and $\Delta S_{f,ox}$ of $Ln_xU_{1-x}O_{2-0.5x+y}$ at lower temperatures instead. Again the differences between $\Delta S_{f,el,T}$ and the room temperature $\Delta S_{f,el,298\ K}$ is necessary for the interpretation and are calculated by Eq. (19) using the same data for Eq. (16),

$$\Delta S_{f,el,T} - \Delta S_{f,el,298\ K} = \int_{298\ K}^{T} \frac{\Delta C_p}{T} dT \quad (19)$$

The $\int_{298\ K}^{T} \frac{\Delta C_p}{T} dT$ terms are determined to be less than 10 J/mol K at 1173–1573 K, generally within 6% of $\Delta S_{f,el,T}$, which makes them good estimates for $\Delta S_{f,el}$. Assuming that $\Delta H_{f,el}$ and $\Delta S_{f,el}$ are constant over 298–1500 K, we can calculate $\Delta H_{f,ox}$ and $\Delta S_{f,ox}$ using Eqs. (17) and (18), using the thermodynamic properties of element and oxides from Ref. [33], and the results are listed in Table 8.

As shown in Table 8, $\Delta H_{f,ox}$ of rare earth doped uranium oxides become increasingly negative when dopant amount increases, which is consistent with the reported data from direct calorimetry. One the other hand, $\Delta S_{f,ox}$ are generally slightly positive for the solid solutions with lower dopants, and is negative for $La_{0.2}U_{0.8}O_2$. This can be explained by the formation of defect clustering which decreases entropy of the system even when more defects are introduced. $\Delta G_{f,ox}$ at 298 K and 900 K are calculated and listed in

Table 6
Estimation of Enthalpies of formation of $Ln_xU_{1-x}O_{2-0.5x+y}$ solid solutions from elements at room temperatures (298 K).

Composition	Fit equation for $\Delta H_{f,el}$ (kJ/mol)
$La_xU_{1-x}O_{2-0.5x+y}$	−1084.9 + 84.0*x − 138.9*y or −807.1 + 14.55*x − 138.9*(O/M)
$Y_xU_{1-x}O_{2-0.5x+y}$	−1084.9 + 28.6*x − 138.9*y or −807.1−40.85*x − 138.9*(O/M)
$Nd_xU_{1-x}O_{2-0.5x+y}$	−1084.9 + 76.9*x − 138.9*y or −807.1 + 7.45*x − 138.9*(O/M)

Note: O/M = 2−0.5x + y.

Table 7
Formation enthalpies and formation entropies at elevated temperatures from free energy measurements and formation enthalpies at room temperatures from fit equations.

Composition	Mean temperature T (K)	$\Delta H_{f,el,T}$ at T (kJ/mol)	$\Delta H_{f,el}$ at 298 K (kJ/mol)	$\Delta S_{f,el,T}$ at T (J/mol·K)	Reference
$La_{0.025}U_{0.975}O_{2.075}$	1523	−1095.62	−1094.95 ± 0.89	−176.98	Hagemark and Broli [12]
$La_{0.05}U_{0.95}O_{2.01}$	1523	−1083.32	−1085.56 ± 0.94	−174.05	Hagemark and Broli [12]
$La_{0.05}U_{0.95}O_{2.10}$	1573	−1098.51	−1098.06 ± 0.85	−179.49	Hagemark and Broli [12]
$La_{0.2}U_{0.8}O_2$	1323	−1104.53	−1081.99 ± 1.11	−197.07	Yoshida et al. [15].
$Y_{0.025}U_{0.975}O_{2.05}$	1523	−1092.65	−1092.87 ± 0.92	−175.31	Hagemark and Broli [12]
$Y_{0.025}U_{0.975}O_{2.20}$	1573	−1116.92	−1113.70 ± 0.77	−187.86	Hagemark and Broli [12]
$Y_{0.048}U_{0.952}O_{2.125}$	1573	−1103.28	−1104.22 ± 0.83	−180.33	Hagemark and Broli [12]

Table 8
Formation enthalpies and formation entropies from constituent oxides ($LnO_{1.5}$, UO_2, and UO_3).

Composition	$\Delta H_{f,ox}$ (kJ/mol)	$\Delta S_{f,ox}$ (J/mol K)	$\Delta G_{f,ox}$ at 298 K (kJ/mol)	$\Delta G_{f,ox}$ at 900 K (kJ/mol)	Reference
$La_{0.025}U_{0.975}O_{2.075}$	−3.60	7.76	−5.92	−10.58	Hagemark and Broli [12]
$La_{0.05}U_{0.95}O_{2.01}$	−3.32	5.23	−4.97	−8.03	Hagemark and Broli [12]
$La_{0.05}U_{0.95}O_{2.10}$	−5.95	7.59	−8.21	−12.78	Hagemark and Broli [12]
$La_{0.2}U_{0.8}O_2$	−43.61	−16.74	−38.62	−28.54	Yoshida et al. [15].
$Y_{0.025}U_{0.975}O_{2.05}$	−2.73	7.38	−4.93	−9.37	Hagemark and Broli [12]
$Y_{0.025}U_{0.975}O_{2.20}$	−6.05	7.35	−8.24	−12.67	Hagemark and Broli [12]
$Y_{0.048}U_{0.952}O_{2.125}$	−4.31	8.90	−6.96	−12.32	Hagemark and Broli [12]

Table 8 as well, all suggesting more favorable formation of solid solutions at higher temperature from the constituent oxides.

The calorimetric studies of rare earth doped uranium oxides demonstrate that adding these cations into the fluorite UO_2 materials leads to a structure strongly stabilized at the oxygen interstitial region. At relatively high p_{O_2}, the defect structure of the hyperstoichiometric $La_xU_{1-x}O_{2-0.5x+y}$ has been suggested to be dominated by complex defect clusters $\{2(O_i''O_i''V_O^{\bullet\bullet})\}$ by electrical conductivity measurements [36]. The observed strongly exothermic enthalpies and smaller formation entropies may reflect the formation of these complex defect clusters. However, a better understanding of the separate effects from oxidation and defect clustering needs of further investigation not only in the hyperstoichiometric but also in the hypostoichiometric $Ln_xU_{1-x}O_{2-0.5x+y}$ materials. In addition, thermochemical studies of the hypostoichiometric $Ln_xU_{1-x}O_{2-0.5x+y}$ materials, if such could be made, would be important for comparisons of their enthalpy terms, as a sharp change in energetics is expected around O/M = 2, thus preventing us from extending the hypothesis beyond O/M < 2.

5. Conclusions

The energetics of the La-, Y-, and Nd-doped uranium oxides have been studied by high temperature oxide melt calorimetry over a wide range of dopant concentrations and oxygen contents. The formation enthalpies of these materials from constituent oxides ($LnO_{1.5}$, UO_2, plus UO_3) become more negative with increasing dopant concentration and are independent of the uranium oxidation states. The oxidation enthalpies of $Ln_xU_{1-x}O_{2-0.5x+y}$ are similar to that of UO_2, though this does not necessarily constrain the actual valence state of the oxidized uranium to be hexavalent. The formation enthalpies from elements are in good agreement with those calculated from free energy data. The deeper understanding of these materials will require more calorimetric studies on the materials covering a wider range, not only in the oxygen excess region, but also in the oxygen deficient region.

Acknowledgments

This work was supported as part of the Materials Science of Actinides, an Energy Frontier Research Center funded by the U.S. Department of Energy, Office of Science, Basic Energy Sciences under Award # DE–SC0001089. L. Zhang thanks T.Y. Shvareva for help on the preparation of lanthanum doped uranium oxide samples. The authors thank Sarah Roeske and Nicholas Botto for help with the electron probe microanalysis.

References

[1] J.K. Fink, J. Nucl. Mater. 279 (2000) 1–18.
[2] D.R. Olander, Fundamental Aspects of Nuclear Reactor Fuel Elements, National Technical Information Services, Springfield, VA, 1985.
[3] T.B. Lindemer, J. Brynestad, J. Am. Ceram. Soc. 69 (1986) 867–876.
[4] P.V. Nerikar, X.-Y. Liu, B.P. Uberuaga, C.R. Stanek, S.R. Phillpot, S.B. Sinnott, J. Phys. Condens. Matter 21 (2009) 1–9.
[5] H. Kleykamp, J. Nucl. Mater. 131 (1985) 221–246.
[6] R.V. Krishnan, G. Panneerselvam, M.P. Antony, K. Nagarajan, J. Nucl. Mater. 403 (2010) 25–31.
[7] H. Kleykamp, J. Nucl. Mater. 206 (1993) 82–86.
[8] W.B. Wilson, C.A. Alexander, A.F. Gerds, J. Inorg. Nucl. Chem. 20 (1961) 242–251.
[9] P. Högselius, Energy Policy 37 (2009) 254–263.
[10] I.W. Donald, B.L. Metcalfe, R.N.J. Taylor, J. Mater. Sci. 32 (1997) 5851–5887.
[11] W.J. Weber, A. Navrotsky, S. Stefanovsky, E.R. Vance, E. Vernaz, MRS Bull. 34 (2009) 46–53.
[12] K. Hagemark, M. Broli, J. Am. Ceram. Soc. 50 (1967) 563–567.
[13] E. Stadlbauer, U. Wichmann, U. Lott, J. Solid State Chem. 10 (1974) 341–350.
[14] T. Fujino, J. Nucl. Mater. 154 (1988) 14–24.
[15] K. Yoshida, T. Arima, Y. Inagaki, K. Idemitsu, M. Osaka, S. Miwa, J. Nucl. Mater.

418 (2011) 22–26.
[16] L. Mazeina, A. Navrotsky, M. Greenblatt, J. Nucl. Mater. 373 (2008) 39–43.
[17] D.C. Hill, J. Am. Ceram. Soc. 45 (1962) 258–263.
[18] M. Aizenshtein, T.Y. Shvareva, A. Navrotsky, J. Am. Ceram. Soc. 93 (2010) 4142–4147.
[19] B.E. Hanken, T.Y. Shvareva, N. Grønbech-Jensen, C.R. Stanek, M. Asta, A. Navrotsky, Phys. Chem. Chem. Phys. 14 (2012) 5680–5685.
[20] T. Fujino, N. Sato, K. Yamada, Fresenius J. Anal. Chem. 354 (1996) 374–375.
[21] A. Navrotsky, Phys. Chem. Min. 2 (1977) 89–104.
[22] A. Navrotsky, Phys. Chem. Min. 24 (1997) 222–241.
[23] K.B. Helean, A. Navrotsky, E.R. Vance, M.L. Carter, B. Effinghaus, O. Krilorian, J. Lian, L.M. Wang, J.G. Catalano, J. Nucl. Mater. 303 (2002) 226.
[24] A. Navrotsky, J. Therm. Anal. Calorim. 57 (1999) 653–658.
[25] R.A. Robie, B.S. Hemingway, U. S. Geol. Surv. Bull. (1995) 2131.
[26] R.D. Shannon, Acta Cryst. A32 (1976) 751–767.
[27] D. Kim, J. Am. Ceram. Soc. 72 (1989) 1415–1421.
[28] Swarthmore, PA, File No 5–550, Joint Committee on Powder Diffraction Standards, 1960.
[29] L. Lynds, W.A. Young, J.S. Mohl, G.G. Libowitz, Adv. Chem. 39 (1962) 58–65.
[30] S. Guillemet-Gritsch, A. Navrotsky, P. Tailhades, H. Coradin, M. Wang, J. Solid State Chem. 178 (2005) 106–113.
[31] A. Navrotsky, J. Inorg. Nucl. Chem. 31 (1969) 59–72.
[32] J. Dicarlo, J. Bularzik, A. Navrotsky, J. Solid State Chem. 96 (1992) 381–389.
[33] L.B. Pankratz, Thermodynamic Properties of Elements and Oxides, 1982.
[34] R.V. Krishnan, V.K. Mittal, R. Babu, A. Senapati, S. Bera, K. Nagarajan, J. Alloy. Compd. 509 (2011) 3229–3237.
[35] V.J. Wheeler, R.M. Dell, E. Wait, J. Inorg. Nucl. Chem. 26 (1964) 1829–1845.
[36] T. Matsui, K. Naito, J. Nucl. Mater. 138 (1986) 19–26.
[37] J.H. Cheng, A. Navrotsky, J. Mater. Res. 18 (2003) 2501–2508.
[38] T.A. Lee, A. Navrotsky, J. Mater. Res. 19 (2004) 1855.
[39] S.V. Ushakov, K.B. Helean, A. Navrotsky, L.A. Boatner, J. Mater. Res. 16 (2001) 2623–2633.
[40] V.P. Glushko, Thermal Constants of Substances, VINITI, Moscow, 1965-1982, pp. 1–10 issued.
[41] B.J. McBride, M.J. Zehe, S. Gordon, NASA Glenn Coefficients for Calculating Thermodynamic Properties of Individual Species, 2002. NASA/TP-2002–211556.